Meteorol. Z. (Contrib. Atm. Sci.), PrePub DOI 10.1127/metz/2019/0924

Electricity production by wind turbines as a means for the verification of wind simulations

Axel Weiter*, Martin Schneider, Dennis Peltret and Heinz-Theo Mengelkamp

anemos Gesellschaft für Umweltmeteorologie, Reppenstedt, Germany

(Manuscript received May 7, 2018; in revised form October 19, 2018; accepted November 21, 2018)

Abstract

Wind measurements are rare in heights of interest in terms of wind turbines. Consequently, well-verified model simulations of the wind conditions are fundamental during the planning stage of wind farms. In this paper, a new approach is presented where data from operational wind turbines is used to verify these wind simulations. Several issues are discussed: model wind speed has to be combined with the power curve from the wind turbine in order to be comparable with the turbine data. Furthermore, in operational mode a turbine does not perfectly perform at any time step. Thus, those time steps have to be identified and replaced by missing values since a model cannot reproduce an unsual turbine operation. In addition, wind turbines are influenced by surrounding turbines resulting in a reduction of power production at some time steps. Consequently, a wake model is applied on the model simulation. In a next step, the edited turbine power data is compared to the power time series resulting from a mesoscale simulation for Germany with the mesoscale model WRF. The simulation is improved by a remodelling-method during the post-processing. This method alters the model wind speed and particularly results in a reduced wind speed bias. Comparing these model simulation's power production time series to the turbine production data reveals that they correlate well with most values in the range of 0.82 to 0.87 for an hourly temporal resolution. The relative bias for the simulations is between 10 to 25 % in terms of power. Finally, a comparison with a model verification with wind measurement data is carried out. It is shown that the verification with data from operational wind turbines and from wind measurements are in the same range in terms of correlations.

Keywords: mesoscale model verification, wind turbine production data, modelling of wind conditions, wind simulation

1 Introduction

Long-term statistical properties of wind conditions (wind speed and direction) as well as short-term forecasts are of interest for environmental (pollutant dispersion, damage by storms), recreational (sailing, gliding flights), and economic (electricity production by wind turbines) applications. In particular, the wind industry with its enormous increase in installed capacity worldwide during the last two decades and its intuitive economic value asks for information on the wind potential on a wide range of temporal and spatial scales. Atmospheric numerical models are used to estimate site specific wind conditions (Troen, 1996) as well as regional-scale (Mengelkamp et al., 1997; Mengelkamp, 1999) to global-scale wind maps (Vaisala 3TIER, 2014). Verification of numerical wind simulations, however, still remains a challenge. Attempts were made to compare simulated wind statistics to observations at weather stations (Kaiser-Weiss et al., 2015) and meteorological towers (Drechsel et al., 2012). However, already Wieringa (1980, 1996) questioned the representativeness of wind speed measurements at weather stations because of the standard height of 10 m and the strong influence of any kind of small obstacle and roughness conditions in the immediate surrounding on the measurements. In addition, Lindenberg et al. (2012) showed that nearly every wind speed time series at a weather station can be considered inconsistent in time, mostly due to the replacement of anemometers or a change of the measurement location or height. Moreover, the scale mismatch between a point measurement and a model grid scale representative parameter remains. Today, mesoscale models seem to be most suitable for the simulation of wind conditions on regional scales. With a horizontal resolution of about a few kilometers numerical considerations require the lowest vertical layer to be roughly 50 m thick. The relation between the wind speed at different heights depends on surface characteristics and atmospheric stability. Any vertical extrapolation from the lowest model level to the observational height of 10 m implies an uncertainty.

Measurements at tall meteorological towers overcome some of the shortcomings of near-surface measurements. Considering 100 m being a typical height for the atmospheric surface layer, the influence of surface characteristics on wind speed measurements above this height is reduced. Therefore, although being point measurements, these data represent an air volume larger than near-surface mesurements, since the wind field at this height is more homogenous. Tall research towers providing multi-year consistent data sets are most appro-

*Corresponding author: Axel Weiter, anemos GmbH, Böhmsholzer Weg 3, 21391 Reppenstedt, Germany, e-mail: axel.weiter@anemos.de

priate for the verification of wind simulations at single locations. However, since the number of tall towers for research purposes is rather limited, these data sets are not sufficient for a general picture of the uncertainty of a country-wide wind atlas.

In some countries, as a consequence of the growing wind industry, the number of tall measurement towers used for commercial purposes increased during the last years. The height of these towers ranges between 60 m in former times and up to 140 m today. Although commonly only in operation for 12 months, data from these towers would be most helpful for the verification of time series simulations of wind speed and direction. There is no official number of these towers as they are privately owned but from our experience as a wind consultant our guess for Germany is around 500, yet with limited data access.

Our study will go a step further and start from the consideration that the number of operating wind turbines in Germany increased to more than 28,675 in 2017 (Deutsche WindGuard, 2018) distributed all over the country. The electricity production of wind turbines can be considered an indirect measure of the wind conditions. The influence of small-scale surface inhomogeneity is reduced at hub heights of more than 100 m for modern wind turbines and the energy production can be considered representative for a high-resolution mesoscale model grid cell as rotor diameters of more than 120 m represent a rather large air volume due to their large rotor swept area. However, cutbacks are many in using wind turbine production data for the verification of wind simulations. The ability of technical devices to transform kinetic energy of the air into electrical energy is limited to an efficiency of 59 % at a maximum according to Betz' law (Betz, 1926). In addition, the cut-in wind speed of a wind turbine is at around 3 ms^{-1}, rated power from which on the energy production is constant is between 12 and 13 ms^{-1}, and cut-out speed is at 25 ms^{-1}. There is no information at the low and high end of the wind speed frequency distribution and the relation between wind speed and energy production is nonlinear in-between. In addition, losses due to wind farm wake effects and reduced operation modes for various reasons (noise reduction during nights, downtimes for animal protection or maintenance work) have to be accounted for when comparing real production data with simulations.

Our intention is to discuss advantages and disadvantages of using wind turbine energy production as a means for the verification of wind simulations and to show results of a preliminary comparison of numerical mesoscale simulations of the wind conditions over Germany with wind turbine production data.

This paper is organised as follows. The next section describes the model data and how the transformation to power data is realized. Section 3 explains the necessary steps for wind turbine data in order to be useable for model verification purposes. In addition, the wind turbine and wind measurement data finally used are described. The results of the verification are presented in Section 4. Section 5 comprises a summary and a brief outlook.

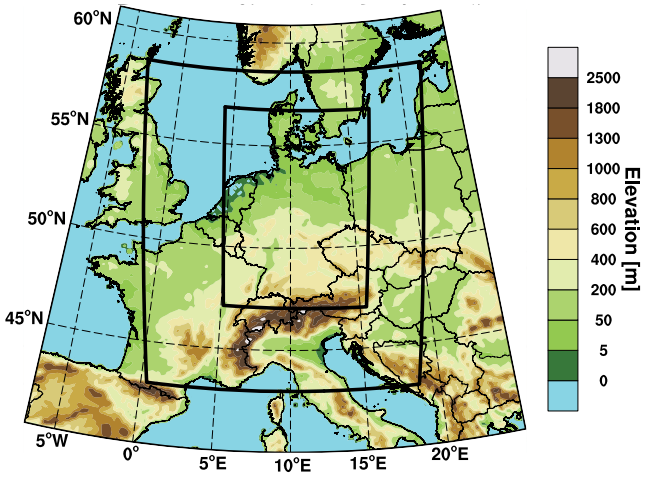

Figure 1: Outer ($15 \times 15\,km^2$ horizontal resolution) and inner ($3 \times 3\,km^2$ horizontal resolution) WRF model domains.

2 Model data

2.1 Mesoscale model simulation

The mesoscale model WRF (Weather Research & Forecasting Model version 3.7.1) (Michalakes et al., 2004; WRF, 2016) is used to downscale MERRA-2 reanalysis data (Molod et al., 2015) to the region of Germany (Figure 1). A detailed description of the model is given by Skamarock et al. (2008). Initial and boundary conditions are taken from MERRA-2 (Molod et al., 2015) and CFSR/CFSv2 (Saha et al., 2014) reanalysis data sets. Orography data are taken from the SRTM data set (Shuttle Radar Topography Mission, USGS EROS Data Center (Farr et al., 2007)), which has a horizontal resolution of 90 m and a vertical resolution of 1 m. No corrections were performed and any uncertainties particularly over forested areas are accepted as we are interested in a countrywide study and our focus is not on site-specific analysis. Vegetation and roughness information is extracted from the CORINE data set of the European Environment Agency (Keil et al., 2010). The horizontal resolution is 100 m and the latest revision is from 2006. Soil temperature, soil humidity and snow cover are taken from the CFSR data set with 4 soil levels. The vertical structure of the model is divided into 25 hybrid levels with model top at 100 hPa. Eight of the 25 vertical levels form the lowest atmospheric layer relevant for wind energy use up to 250 m height with 20 m distance up to 200 m height.

A two-way nesting strategy is realized to step down from the MERRA-2 resolution of approximately $50 \times 50\,km^2$ over Germany with a horizontal resolution of $15 \times 15\,km^2$ in the outer model domain to the

$3 \times 3\,\mathrm{km}^2$ grid of the inner domain. Every 3 hours both model domains are nudged towards wind (u,v), temperature and specific humidity from MERRA-2 reanalysis data. Nudging is only applied beyond the planetary boundary layer.

WRF's physics parameterization considers the Yonsei University (YSU) planetary boundary layer scheme, the Monin-Obukhov surface layer description, the Noah land surface model including Mosaic 4, the RRTM scheme for the longwave radiation and the Dudhia parameterization for the short-wave radiation. No cumulus parameterization is applied (Skamarock et al., 2008).

The time-period 1997 to 2017 is simulated and relevant variables are stored every 10 minutes.

2.2 Remodelling

An optimization approach (called 'Remodelling' in the following) is applied to the wind speed time series of the lowest levels up to 200 m of the standard WRF simulation. The general idea of this remodelling step is to use sub-grid information which is not part of the original WRF simulation to improve the wind speed model output. The remodelling is based on the comparison of simulated wind speed time series with observations in the height range of 80 to 140 m. In the subsequent first verification, data from 45 towers were used. During the remodelling process, data from 28 of them were used for training. The remodelling basically consists of four steps:

(1) An elevation correction for wind speed is applied on the model data that accounts for speed-up effects over unresolved crests (Howard and Clark, 2007). This correction accounts for the height difference Δh between the elevation above sea level of a particular measurement site and the average elevation of the model grid cell of $3 \times 3\,\mathrm{km}^2$. It changes the original model wind speed output u_{WRF} to the corrected wind speed u_{WRF*} via

$$u_{WRF*} = u_{\mathrm{WRF}} \cdot (1 + \Delta h \cdot r) \qquad (2.1)$$

with r being a constant in units of m^{-1} empirically derived from simulations with a high resolution computational fluid dynamics (CFD) code.

(2) In a second step, both modeled u_{WRF*} and observed u_{obs} wind speed data with a resolution of 10 min are separated into eight wind direction sectors to account for various surface characteristics within these sectors. A linear regression analysis $u_{\mathrm{obs}} = m \cdot u_{WRF*} + b$ follows for simulated and observed wind speed providing regression coefficients for each measurement site and 8 wind direction sectors, respectively.

(3) There are now 16 regression coefficients for each of the 28 measurement sites (offset and slope of the regression line for each of 8 wind direction sectors). A multiple linear regression analysis is now performed separately for slope and offset parameters taking into account sub-grid information on orography (x_1) (height of grid cell) and height gradient (x_2), latitude (x_3) and surface roughness (x_4)

$$m' = c_0 + c_1 \cdot x_1 + c_2 \cdot x_2 + c_3 \cdot x_3 + c_4 \cdot x_4 \qquad (2.2)$$

and similar for b'. The goal of this step is the calculation of global slope-parameters (c_i) for any type of sub-grid information (x_i) from the training data.

(4) With the global parameter derived from the 28 training met masts scaling factors are calculated for the wind speed at each model grid cell taking into account the respective sub-grid information. The scaling factors are applied for each wind direction sector and result in a corrected simulated wind data set.

As a result of the remodelling process the bias of the mean wind speed at all 45 met masts (Figure 2) is reduced. Before the remodelling process the model showed a positive bias (model winds were too strong) for all onshore met masts of up to 30 % and a negative bias of about 5 % for offshore conditions. After the remodelling process the bias is between −10 % and +10 % for onshore masts and almost zero for the offshore sites. The verification data set is not totally independent from the data used for the remodelling as the 28 towers used for the remodelling process are among the 45 shown in Figure 2. This seems to be justified as first, the simulated data are corrected by global scaling factors based on the analysis of all 28 towers and second, Figure 2 does not reveal any difference in model skill considering masts used in the remodelling and those, which are not.

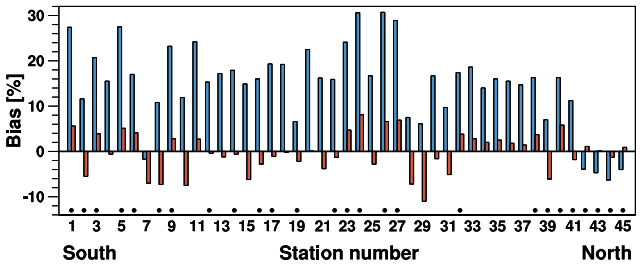

Figure 2: Bias of simulated wind speed in comparison to wind speeds measurements from 45 met masts (100 m height) before (blue) and after (red) the remodelling process. The black dots indicate the wind speed measurements used in the remodelling.

2.3 Making simulated wind speed data comparable to wind turbine output

Instead of using wind speed measurements for the verification we follow the idea of using data from operational wind turbines. More than 28,000 turbines distributed all over Germany were in operation in 2017 (Deutsche WindGuard, 2018). Hub heights meanwhile reach more than 150 m which reduces the influence of surface characteristics on the power production. With rotor diameters of more than 150 m the power output cannot be considered a point measurement but rather represents an air volume passing through a plane of almost 20,000 m^2.

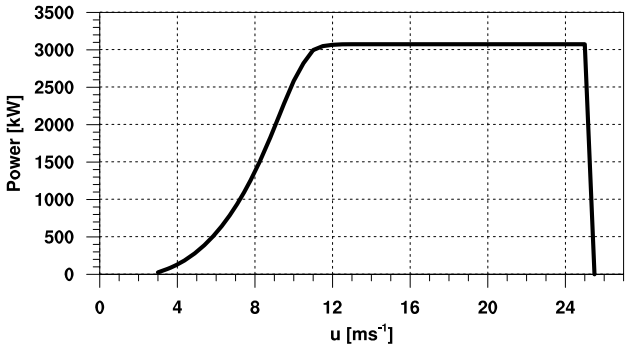

Figure 3: Power curve of a typical 3,000 kW wind turbine.

Opposed to these advantages are major shortcomings. Power output is connected to wind speed via

$$E = \sum_{u_j=u_{in}}^{u_c} P(u_j) \cdot f(u_j) \cdot 8760 \qquad (2.3)$$

where E [kWh] is power production in a year's time (8760 hours), $P(u_j)$ [kW] the power at wind speed u_j [ms^{-1}] and $f(u_j)$ the wind speed frequency distribution. u_{in} and u_c are cut-in speed and cut-out speed, respectively. From the power curve (Figure 3) it is obvious that the power output does not comprise any information on the wind conditions below cut-in speed (the wind speed at which a turbine starts operating, usually around 3 to 4 ms^{-1}) and above cut-out speed (the wind speed at which a turbine stops operation, usually at around 25 ms^{-1}). From rated wind speed (the wind speed at which a turbine reaches its maximum (rated) power, often between 11 and 13 ms^{-1}) to cut-out speed there is only bulk information as the turbine keeps its power output at a constant level. With the power of the undisturbed wind flow $P_0 = \frac{1}{2}\rho F u^3$ (ρ is air density and F the rotor swept area) and the power coefficient of the turbine c_p, the turbine's power is

$$P = c_p \cdot P_0 \qquad (2.4)$$

with a maximum value of 0.59 for c_p according to Betz' law. Because of the non-linearity between wind speed and power output the verification is indeed for the variable wind power rather than for wind speed. However, since the model simulation verified here is mainly used for the estimation of wind turbine electricity production, it seems reasonable to compare the electricity production rather than wind speed. Equation 2.4 also indicates that only a part of the wind power is transformed into electrical power.

Another complicating factor regarding this transformation is the fact that the kinetic energy of the air flow depends on air density and consequently, the power curve of a wind turbine depends on air density as well. This issue can be overcome by either using a density specific power curve or by correcting the wind speed to standard density $\rho_0 = 1.225\,\mathrm{kg\,m^{-3}}$ via

$$u_{\rho_0} = u\left(\frac{\rho}{\rho_0}\right)^{\frac{1}{3}} \qquad (2.5)$$

which is applied to the simulated wind speed time series. Air density is calculated from model variables pressure and temperature via the barometric formula and ideal gas law. The uncertainty of the modeled air density is part of the overall uncertainty of the power output simulation.

In this paper, the technical transformation from wind speed to power is accounted for by combining the density-corrected model wind speed time series at hub height every 10-minute time step with the measured power curve of the respective wind turbine. Thus, the verification is performed on simulated model based power output and real power output from operating turbines. Due to the dependence on the 3rd power of the wind speed, the comparison of power is more sensitive to any uncertainty than a comparison of the wind speed itself. From our experience a factor of 2.5 seems realistic for the transformation of the uncertainty in wind speed to the uncertainty in electricity production.

However, this transformation results in the turbine yield without any losses, i.e. in this first step, it is assumed that the turbine operates in its optimal technical mode and is not influenced by any wake effects from neighbouring turbines. These assumptions, however, are hardly given as most turbines are part of a wind farm and operate under mode restrictions and external interferences. Individual restrictions and not foreseeable failures cannot be accounted for a priori by the simulations but these are detected by the analysis of operational data described in Section 3. Wake effects are considered by applying a simple wake model that only accounts for the most general processes and does not treat the time-variable influence of wind shear, stratification and turbulence.

The wake loss for a particular wind turbine is calculated at any time step of 10 min and is applied to the wind speed time series before it is combined with the respective power curve. Wake effects crucially depend on wind direction which could be taken from the turbine orientation. But this process would mix simulated and operational data and the accuracy would depend on the often imprecise turbine orientation to the north. Consequently, wind direction for wake effect calculation is taken from WRF simulations.

The wake model is based on the equation for cluster efficiency by Katic et al. (1986) and reduces the wind speed allocated to each respective turbine location:

$$\delta u = u_0(1 - \sqrt{1 - c_t})\left(\frac{D_0}{D_0 + 2k_w s_{01}}\right)^2 \frac{A_{ov}}{A_1} \qquad (2.6)$$

δu is the effective wind speed deficit at turbine 1 caused by turbine 0 (Figure 4) which faces wind speed u_0. The thrust coefficient c_t describes the influence of a wind

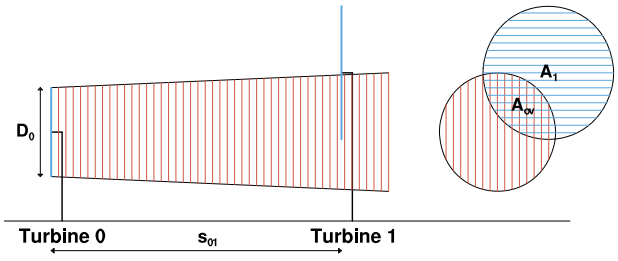

Figure 4: Schematic of the wake effect. The red pattern indicates the area influenced by turbine 0, the blue pattern shows the rotor area (A_1) of turbine 1. A_{ov} indicates the overlapping area. Adapted from DTU Wind Energy.

turbine on the flow field and is provided by the manufacturer. D_0 represents the rotor diameter of turbine 0, s_{01} the horizontal distance between both turbines, and the wake decay constant k_w describes how fast the wake decays and how strong it expands over a certain distance. k_w is considered to depend on surface roughness only and ranges from 0.04 for water surfaces to 0.1 for forested areas and cities. Time-varying thermally induced turbulence and any other time-varying influence are neglected here and since data from time periods of one year and longer is considered, the time-varying influence should be averaged out. Also the geometry of the wind turbines is important as depending on the rotor diameter, hub height, distance, and wind direction only a partial overlap of the rotor swept area may happen.

The percentage of the rotor area affected by the wake is calculated from the geometry of the turbines, the distance and wind direction every 10-min time step. If a turbine is affected by the wake of several turbines simultaneously, the overall wake effect is calculated as the square root of the individual wake effects squared following Katic et al. (1986). This simple wake model is compared with the integrated wake model of the commercially available Meteodyn Computational Fluid Dynamics model (Meteodyn, 2012). The difference in wind speed reduction for a 6-turbine wind farm is less than 10 % (wake effect by Meteodyn 3.9 %, by our wake model 4.3 %) on average and in power less than 4 % (Meteodyn 9.8 %, our wake model 10.2 %) on average. Given the general uncertainty in wind farm wake modelling and in comparing operational and simulated turbine power data this difference is acceptable.

3 Observational data

3.1 Electricity production by operational wind turbines

The general idea to use data from wind turbines for mesoscale model verification results from the fact that wind measurements are quite rare in particular at larger heights with reduced influence of surface characteristics. Furthermore, the wind industry is interested in power output of wind turbines rather than wind speed.

SCADA (Supervisory Control and Data Acquisition) data sets from operational wind turbines comprise a large number of operational parameters of each wind turbine. Wind speed measured by an anemometer mounted on the nacelle behind the rotor is also provided by the data sets. However, this anemometer is strongly influenced by turbulence generated by the rotor blades and also experiences a wind speed deficit since the rotor is extracting energy from the flow. Consequently, this wind speed data have little resemblence to the wind conditions. These data meant for turbine control is also post-processed by the turbine manufacturer and not provided as raw data. Thus, the wind speed data from the nacelle anemometer is not used for verification purposes. This paper focuses on turbine power output. Nevertheless, the wind speed data are useful during the filtering process of the power output described in the following.

We aim at using the electricity production of an operating wind turbine for mesoscale model verification. A wind turbine hardly operates in an optimal mode but is affected by technical losses e.g. shut down for maintenance work and electrical grid losses as well as intentionally reduced operation during certain times because of regulatory restrictions for noise reduction and animal protection (commonly bats and birds). Consequently, turbine power data have to be filtered very precisely in order to obtain a data set that only includes values the mesoscale model is able to reproduce. The filtering process is based on a detailed analysis of SCADA data, which are typically stored with a 10 min time step. All time steps indicating an error by the turbine itself are removed and additional incorrect data are filtered out identified using a wind speed vs. power diagram drawn from operational data. At this point wind speed data from the nacelle is used after being transformed by a transfer function provided by the turbine manufacturer. Although not exact, these data are acceptable for filtering power data. Filtering removes all values that are basically off the triple standard deviation marked by the purple lines in Fig. 5. The filtering process adds a certain amount of missing values to the production data set. In order to realize a consistent statistical analysis the corresponding data in the modeled time series are marked as missing values as well.

3.2 Wind farm data used for verification

Production data from 50 turbines in 12 wind farms are used for verification purposes (Table 1, access to data was given for a selection of turbines only in some wind farms). These data are averaged to a temporal resolution of 10 min. The wind farms are more or less arbitrarily distributed within the model domain and represent complex and simple surface characteristics. In order to extract the most appropriate time series for comparison with observational data the nearest neighbor method is applied simply using the model grid point closest to the turbine site. A bilinear interpolation using the four closest grid points and a weighted average showed similar

Table 1: Wind farms used for the verification.

Wind farm	Turbine Type	No. of turbines	Period	Hub height [m]	Orography	Land use
A	Enercon E82	2	11/2011–10/2016	138	Flat	Mixed Farmland
B	Nordex N117	5	01/2015–12/2016	120	Flat	Mixed Farmland
C	GE 1.5sl	2	01/2012–12/2012	100	Flat	Mixed Farmland
D	Enercon E82	2	01/2015–12/2016	108	Flat	Mixed Farmland
E	Vestas V112	6	01/2013–10/2016	94	Flat	Mixed Farmland
F	Nordex N117	6	10/2015–10/2016	141	Flat	Forest and Villages
G	Enercon E82, E101	2	01/2013–12/2016	98, 135	Flat	Trees and Farmland
H	Enercon E82	2	12/2014–09/2016	85, 98	Flat	Trees and Farmland
J	Vestas V112	5	03/2014–09/2016	140	Complex	Forest and Villages
K	GE 2.5	6	11/2015–12/2016	139	Complex	Trees and Farmland
L	Enercon E101, E126	11	03/2013–02/2016	135	Complex	Forest and Villages
M	Vestas V90	1	09/2015–12/2016	105	Complex	Trees and Farmland

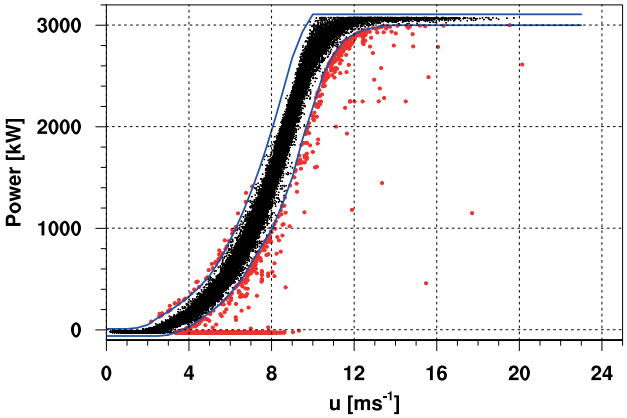

Figure 5: Power curve from operational data for filtering. Black (red) dots indicate valid (invalid) data seperated by blue lines.

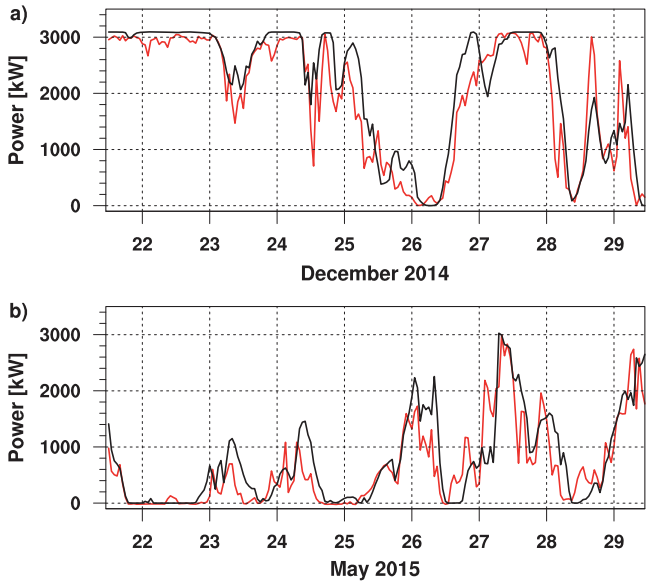

Figure 6: Energy production time series of an operational wind turbine with 3.1 MW rated power (red) from wind farm J and the corresponding simulated electricity production (black). (a) shows hourly data for the period 22 to 29 December 2014 and (b) for the period 24 to 31 May 2015.

skill but is not superior. In the vertical, wind speed is linearly interpolated onto hub height between model levels. Linear interpolation is preferred over the more complex logarithmic interpolation method since the difference of both methods is negligible at heights around 100 m.

3.3 Wind measurement data

It is not the intention of this paper to focus on wind measurements at meteorological towers. These data are only used to compare the model verification results of wind turbine data, which are presented in the following section, with verification results from a common verification method (e.g. model verification with wind measurements). In total, 46 wind speed measurements from towers and LiDARs providing averages of 10 min are used, all of them including at least one year of measurement. Measurement heights from 80 to 160 m are selected since this is the range of the hub heights of the wind turbines providing the data.

4 Results

This paper intents to demonstrate the idea of using data from operating wind turbines for the verification of wind simulations. When comparing production data from operating wind turbines with model simulations, the higher uncertainty has to be considered in contrast to a comparison of wind speed.

Hourly-averaged time series (from six 10 min values) for the energy production from an operating wind turbine and its simulated counterpart are shown in Figure 6 for a typical high wind speed period (winter months in northern Europe, Figure 6a) and for a typical low wind speed period (summer months in northern Europe, Figure 6b). During the high wind speed period, the simulated output often reaches rated power of 3.1 MW while the maximum output of the real operating turbine is always lower than rated power. Wind farm wake effects and/or technical reasons may account for this difference. There are short periods with larger differences between simulated and real power output but in general

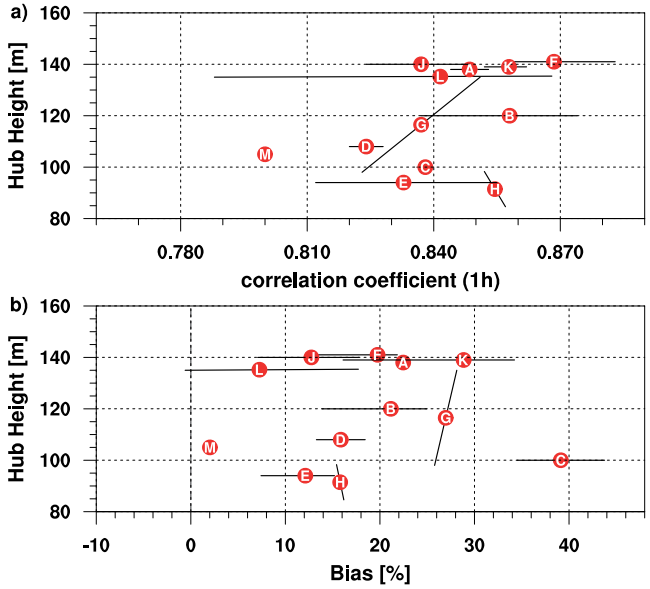

Figure 7: (a) Spearman's correlation coefficient (1 h) beetween simulated and measured power from wind turbines and (b) relative bias of the simulated power. For both statistical parameters, the wind farm average is indicated by the red dot. Black lines mark the range between the maximum and the minimum of a wind farm. Note that the vertical bars occur due to different hub heights within one wind farm. Since wind speed and power are not normally distributed, Spearman's rank correlation coefficient, which is a distribution-free statistic, is preferred over the more common Pearson correlation coefficient, which is not.

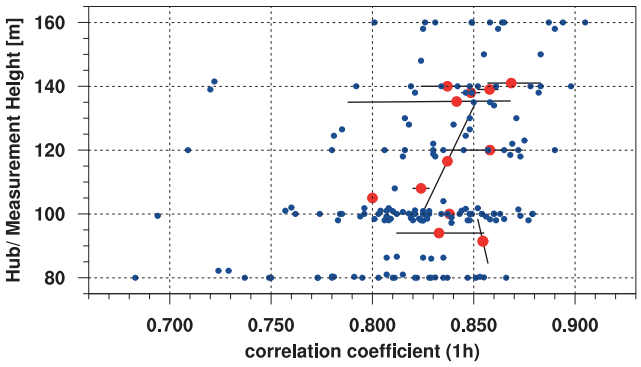

Figure 8: Red dots illustrate the average correlation coefficients of a wind farm, which were shown as wind farm average in Figure 7a. Blue dots indicate Spearman's correlation coeffiecients between simulated and measured wind speed from wind measurement towers and LiDARs. In total, 46 wind speed measurements were used. Many of them provide several measurement heights.

the hourly temporal variability matches well with a correlation coefficient of 0.91. The statement also holds for the low wind speed period which, however, shows larger differences at first glance. The correlation coefficient of the summer period is 0.84.

For all analysed turbines the correlation for hourly averages ranges between 0.79 and 0.89 (Figure 7a) with the majority between 0.82 and 0.87. From our experience of comparing wind speed time series from several simulation models with observations, correlation coefficients in this range for hourly data are reasonable. In addition, there is a slight positive trend towards higher correlations with increasing height. The larger the vertical distance to the ground, the more the influence of the surface decreases. Since micro-scale surface roughness changes are underrepresented in the model simulation, model skill generally increases with height and results in the observed increase of correlation with height.

The relative bias (Figure 7b) ranges between 10 % and 25 % for the bulk of the data. In terms of wind speed this would mean a bias of 4 % to 10 % for the annual mean. We have found a general overestimation of power output by model simulations despite the fact that the remodelling process has minimized the uncertainty in wind speed simulations with a positive and negative bias close to zero (Figure 2). We can only speculate whether turbulence or the vertical wind speed profile or other effects in the transformation from wind speed to power output are reason for the effect of overestimation. A more detailed analysis and a discussion with technicians is needed on this issue. The absolute value of the bias is acceptable. Our experience from a large number of site specific energy production assessments shows uncertainties in the range of 10 % for flat terrain to 20 % for complex terrain. A countrywide wind- or production-atlas may not replace site-specific evaluations but the uncertainty may come close.

The data sample yet is too small for a more detailed interpretation. However, a simple comparison with model verification results from wind speed data was carried out. Figure 8 shows correlation coefficients between the same WRF model simulation as used before and wind speed data from 46 measurement sites. Furthermore, the correlation coefficients from the operating wind turbines from Figure 7a are included as well. The comparison demonstrates that results for both types of verification, with wind speed and with electricity production data, are in the same range. This is at least one indicator that the quality of wind turbine data may be high enough in order to be used for model verification.

An analogous investigation of the bias is not meaningful due to the higher uncertainty of electricity production data in contrast to wind speed data (enhanced by a factor of approx. 2.5). This issue is not valid for the correlations.

5 Conclusion and outlook

This paper aims at bringing up the idea and describing a first attempt to use production data from operating wind turbines for the verification of wind field simulations. We used a remodelled WRF simulation with a horizontal resolution of $3 \times 3\,\mathrm{km}^2$ and a temporal resolution of 10 min. We suggested the following steps to make SCADA data from operating wind turbines usable for the verification of model simulations:

a) Filter SCADA data for unplausible values.

b) Extract the corresponding model time series and interpolate to hub height of the respective wind turbine.

c) Apply a (simple) wake model on the model wind speed time series that accounts for wake loss due to other wind turbines.

d) Apply a density correction for wind speed in order to account for the dependency of power curves on air density.

e) Combine the resulting model wind speed time series at every time step (10 min) with the corresponding measured power curve in order to get a time series of simulated production data.

f) Finally compare the time series from step a) with the time series from step e) in order to verify the model simulation.

The approach was applied to 50 turbines in 12 wind farms. An extract of the time series of an exemplary wind turbine showed that for both, a summer and a winter period, the hourly temporal variability matches well with correlation coefficients of 0.91 and 0.84, respectively. Furthermore, it was demonstrated that correlation coefficients from 12 wind farms are in the same range as coefficients from 46 wind speed measurement sites (Figure 8). In a last step, it was shown that almost all simulated production data is positively biased. We can only speculate whether this results from the transformation of wind speed to power output or arises due to turbulence or flow inclination. Other possible reasons are a poorly simulated vertical wind profile or the fact that a wind turbine is not oriented perfectly perpendicular to the flow field at any time. This issue is subject for further investigations.

However, the reason the model simulation is calculated for has to be kept in mind. It is mainly used to estimate the power production of wind turbines for the next 20 years. Thus, the idea seems reasonable to use power data of turbines that are already in operation for model verification.

We have highlighted drawbacks, challenges, and methods of using wind turbine production data for the verification of wind field simulations with yet a limited set of data. A sophisticated analysis of SCADA data is necessary in order to accept the turbine production data as a reliable means for the wind conditions and a common understanding of wind turbine operation and mesoscale numerical modelling is mandatory. However, the number of wind turbines and their large hub height and rotor diameter are advantageous compared to standard weather station wind measurements and may make the effort worthwhile.

Acknowledgements

This paper is based on data provided by wind farm owners. Furthermore, the study was partly supported by N-Bank Niedersachsen in the framework of the VERIMA project. Special thanks go to DTU Wind Energy for providing us their figure. The final form of this paper also benifited from the helpful comments and suggestions of the anonymous reviewers.

References

Betz, A., 1926: Wind-Energie und ihre Ausnutzung durch Windmühlen. – Vandenhoeck & Ruprecht, Göttingen.

Deutsche WindGuard, 2018: Status des Windenergieausbaus an Land in Deutschland. – Available online: https://www.windguard.de/windenergie-statistik-jahr-2017.html? (accessed on October 16, 2018).

Drechsel, S., G.J. Mayr, J.W. Messner, R. Stauffer, 2012: Wind speeds at heights crucial for wind energy: Measurements and verification of forecasts. – J. Appl. Meteor. Climatol. **51**, 1602–1617, DOI:10.1175/JAMC-D-11-0247.1.

Farr, T.G., P.A. Rosen, E. Caro, R. Crippen, R. Duren, S. Hensley, M. Kobrick, M. Paller, E. Rodriguez, L. Roth, D. Seal, S. Shaffer, J. Shimada, J. Umland, M. Werner, M. Oskin, D. Burbank, D.E. Alsdorf, 2007: The shuttle radar topography mission. – Rev. Geophys. **45**, published online, DOI:10.1029/2005RG000183.

Howard, T., P. Clark, 2007: Correction and downscaling of NWP wind speed forecasts. – Meteor. Appl. **14**, 105–116, DOI:10.1002/met.12.

Kaiser-Weiss, A.K., F. Kaspar, V. Heene, M. Borsche, D.G.H. Tan, P. Poli, A. Obregon, H. Gregow, 2015: Comparison of regional and global reanalysis near-surface winds with station observations over Germany. – Adv. Sci. Res. **12**, 187–198, DOI:10.5194/asr-12-187-2015.

Katic, I., J. Højstrup, N.O. Jensen, 1986: A Simple Model for Cluster Efficiency. European Wind Energy Association.

Keil, M., M. Bock, T. Esch, A. Metz, S. Nieland, A. Pfitzner, 2010: CORINE Land Cover Aktualisierung 2006 für Deutschland. Abschlussbericht zu den F+E Vorhaben UBA FKZ 3707 12 200 und FKZ 3708 12 200.

Lindenberg, J., H.T. Mengelkamp, G. Rosenhagen, 2012: Representativity of near surface wind measurements from coastal stations at the German Bight. – Meteorol. Z. **21**, 99–106, DOI:10.1127/0941-2948/2012/0131.

Mengelkamp, H.T., 1999: Wind Climate Simulation over Complex Terrain and Wind Turbine Energy Output Estimation. – Theor. Appl. Climatol. **63**, 129–139, DOI:10.1007/s007040050098.

Mengelkamp, H.T., H. Kapitza, U. Pflüger, 1997: Statistical-dynamical downscaling of wind climatologies. – J. Wind Eng. Ind. Aerodyn. **67–68**, 449–457, DOI: 10.1016/S0167-6105(97)00093-7.

Meteodyn, 2012: Technical note -meteodyn WT. – Technical report.

Michalakes, J., J. Dudhia, D. Gill, T. Henderson, J. Klemp, W. Skamarock, W. Wang, 2004: The Weather Reseach and Forecast Model: Software Architecture and Performance. – In: Use of High Performance Computing in Meteorology, 156–168, DOI:10.1142/9789812701831_0012.

Molod, A., L. Takacs, M. Suarez, J. Bacmeister, 2015: Development of the GEOS-5 atmospheric general circulation model: Evolution from MERRA to MERRA2. – Geosci. Model Dev. **8**, 1339–1356, DOI:10.5194/gmd-8-1339-2015.

Saha, S., S. Moorthi, X. Wu, J. Wang, S. Nadiga, P. Tripp, D. Behringer, Y.T. Hou, H.Y. Chuang, M. Iredell, M. Ek, J. Meng, R. Yang, M.P. Mendez, H. Van Den Dool, Q. Zhang, W. Wang, M. Chen, E. Becker, 2014: The NCEP climate forecast system version 2. – J. Clim. **27**, 2185–2208, DOI:10.1175/JCLI-D-12-00823.1.

Skamarock, W.C., J.B. Klemp, J. Dudhia, D.O. Gill, D.M. Barker, M.G. Duda, X.Y. Huang, W. Wang, J.G. Powers, 2008: A Description of the WRF Vesion 3. Technical report, National Center for Atmospheric Research Boulder, Colorado, USA.

Troen, I., 1996: The WAsP code. – In: D. Lalas and C.F. Ratto (Eds.), Model. Atmos. flow fields, World Scientific, 435–452.

Vaisala 3TIER, 2014: global wind map available online: https://www.vaisala.com/en/lp/free-wind-and-solar-resource-maps (accessed on October 16, 2018).

Wieringa, J., 1980: Representativeness of Wind Observations at Airports. – Bull. Am. Meteorol. Soc. **61**, 962–971, DOI: 10.1175/1520-0477(1980)061<0962:ROWOAA>2.0.CO;2.

Wieringa, J., 1996: Does representative wind information exist?. – J. Wind Eng. Ind. Aerodyn. **65**, 1–12, DOI: 10.1016/S0167-6105(97)00017-2.

WRF, 2016: User's Guides for the Advanced Research WRF (ARW) Modeling System, Version 3.